Chemistry, Technology and Application of Substances

Vol. 7, No. 1, 2024

Yu. V. Sukhatskyi[1], M. A. Sozanskyi[2], M. V. Shepida[1], Z. O. Znak[1], S. V. Khomyak[3]
Lviv Polytechnic National University,
[1] Department of Chemistry and Technology of Inorganic Substances,
[2] Department of Physical, Analytical and General Chemistry,
[3] Department of Technology of Biologically Active Substances, Pharmacy and Biotechnology
yurii.v.sukhatskyi@lpnu.ua

SYNTHESIS OF SPINEL $MgMn_2O_4$ NANOPARTICLES BY THE CO-PRECIPITATION METHOD IN AN ULTRASONIC FIELD

https://doi.org/10.23939/ctas2024.01.052

Nanoparticles of spinel $MgMn_2O_4$ were synthesized using the co-precipitation method in an ultrasonic field. It was established that at a calcination temperature of 200 °C, all peaks on the diffractogram of the synthesized material corresponded to spinel $MgMn_2O_4$ with a cubic lattice, pronounced crystallinity, and the absence of other phases. As the calcination temperature increased, the formation of new phases – Mn oxides (respectively, Mn_5O_8 and Mn_2O_3) – was recorded. The average size of $MgMn_2O_4$ particles was calculated from the diffraction peaks using the Debye-Scherrer equation and equated to 24.4 nm at a calcination temperature of 200 °C. An increase in the specific power of the ultrasonic processing of the reaction medium revealed a natural increase in the proportion of the amorphous phase and a decrease in the average size of $MgMn_2O_4$ particles.

Key words: spinel; nanoparticles; co-precipitation method; ultrasonic field; Debye-Scherrer equation; average crystallite size.

Introduction

Spinels are materials with the general formula AB_2O_4, where A = Zn^{2+}, Mg^{2+}, Cu^{2+}, Co^{2+} and B = Co^{3+}, Mn^{3+}, Al^{3+}, Fe^{3+}, or other metals [1]. Nanoscale spinels have many practical applications. Thus, nanocrystalline ferrites with a spinel structure are used as catalysts in gas sensors, magnetic information carriers, energy storage devices (supercapacitors), magnetic hyperthermia, and controlled drug delivery systems [2]. Possible areas of application of $MnFe_2O_4$ nanoparticles and other Mn-containing spinels include the following: production of lithium-ion batteries, heavy metal adsorption processes, high-speed generation of hydrogen due to thermochemical decomposition of water [3]; heterogeneous activation of oxidants (hydrogen peroxide, peroxymonosulfates) in the processes of degradation of dyes [4–6], benzyl alcohol [7], bisphenol A [8, 9], antibiotics (erythromycin, tetracycline, amikacin, ofloxacin) [10, 11]; inactivation of microorganisms – gram-positive bacteria (*Staphylococcus aureus*, *Streptococcus pneumonia*), gram-negative bacteria (*Pseudomonas aeruginosa*, *Salmonella paratyphi*), fungi (*Candida albicans*) [7].

The method and conditions of synthesis determine the size, morphology, purity, and crystallinity of $MnFe_2O_4$ spinel nanoparticles, their stability and electromagnetic characteristics [3, 12]. The most common methods of $MnFe_2O_4$ synthesis include [3, 12, 13] the co-precipitation method, solvothermal, hydrothermal, sol-gel methods, thermal decomposition, microemulsion, polyol, template synthesis, the solid-phase reaction method, etc. The advantages of the co-precipitation method include its simplicity, low cost, low temperature and short duration of synthesis, as well as high ability to obtain homogeneous particles of metal multioxides [12, 13].

Catalysts of the spinel type, which contain transition elements (metals) with a 3d-sublevel and a second metal, are more active and stable in advanced oxidation processes due to the synergistic effect of the two oxides, compared to monooxides. Thus, spinel $MgMn_2O_4$ was synthesized using the co-precipitation method, which demonstrated high

catalytic activity during the activation of sodium periodate in the process of oxidative degradation of bisphenol A [1]. The degree of degradation of bisphenol A was equal to 96.17 % due to the use of the $MgMn_2O_4/NaIO_4$ system for 60 minutes. The conditions of oxidative degradation were as follows: reaction volume – 100 mL; pH of the environment – 7.00; temperature – 20 °C; concentration of bisphenol A – 10^{-5} mol/L; concentration of $NaIO_4$ – 10^{-3} mol/L; concentration of $MgMn_2O_4$ is 0.1 g/L. Magnesium oxide, which is part of the spinel, is widespread in nature and has low toxicity in water bodies. Therefore, $MgMn_2O_4$ is an environmentally friendly catalyst that can be used to activate oxidizing agents.

Ultrasound is a method of targeted influence on the morphology and size of spinel particles during their synthesis. Therefore, **the aim of the work** was to study the structural and phase characteristics of $MgMn_2O_4$ spinel particles synthesized by the co-precipitation method in an ultrasonic field.

Materials and research methods

The synthesis of $MgMn_2O_4$ spinel nanoparticles was carried out using the method of co-precipitation in an ultrasonic (US) field. Magnesium nitrate hexahydrate ($Mg(NO_3)_2 \cdot 6H_2O$) and manganese (II) nitrate hexahydrate ($Mn(NO_3)_2 \cdot 6H_2O$) were used as precursors for the synthesis. First, $Mg(NO_3)_2 \cdot 6H_2O$ and $Mn(NO_3)_2 \cdot 6H_2O$ were dissolved in 300 mL of distilled water in a molar ratio of 1:2 with constant stirring. Then the solution was heated to 75 °C in a water bath, the ultrasonic oscillation generator was turned on, and a precipitation agent (aqueous solution of sodium hydroxide with a concentration of 2 mol/L) was added dropwise with constant stirring until the pH value of the reaction medium equated to 9.00. After that, the effect of the ultrasound field on the reaction medium and the addition of drops of sodium hydroxide was stopped. The resulting suspension, which contained light brown particles, was stirred for 2 hours at a temperature of 75 °C to ensure complete crystallization and growth of nanoparticles. To obtain a pure product that does not contain unwanted impurities, the synthesized materials were washed three times with distilled water and three times with ethanol until the pH value equated to 7.00, then separated from the liquid phase by centrifugation (duration – 5 min; frequency – 5000 rpm), and dried at a temperature of 60 °C for 12 hours. The obtained nanoparticles were annealed in an air atmosphere at different temperatures (respectively, 200, 400, 600, and 800 °C) for 5 h. with a heating rate of 5 °C/min.

A magnetostriction-type emitter (Bandelin Sonopuls HD 2200.2, Germany) was used as a generator of US-oscillations (frequency – 20 kHz). The specific power of ultrasonic processing of the reaction medium varied from 200 to 600 W/dm^3. The pH values were monitored with an ADWA AD1200 ATC pH meter with a combined glass electrode and thermocompensator.

The phase composition, average crystallite size, and crystal lattice parameters of the samples under different synthesis conditions were studied by X-ray diffraction (XRD) using an AERIS Research diffractometer (Malvern PANalytical, Great Britain) with Cu Kα radiation (λ = 1.5406 Å). The average crystallite size (D, nm) of the synthesized materials was estimated using the Debye-Scherrer equation [13, 14]:

$$D = \frac{k\lambda}{\beta\cos\theta}, \quad (1)$$

where k is Scherrer's constant, which depends on the Miller index, the index of the reflection plane and the shape of the crystal (usually, k = 0.9); λ is the wavelength of X-radiation (λ = 1.5406 Å); β is the full width at half maximum of the reflection peaks, rad.; θ – diffraction angle (Bragg angle), rad.

Checking the mass and atomic fractions of Mg, Mn, and O in the obtained samples was carried out by the method of energy dispersive X-ray analysis (EDAX) using the X-ray fluorescence analyzer ElvaX Pro (Elvatech, Ukraine).

The scanning electron microscopy (SEM) method was used to study the morphology of the synthesized samples (Tescan Vega 3 LMU electron microscope (TESCAN Brno s.r.o., Czech Republic), equipped with SE- (surface topographic contrast) and BSE-detectors (phase electron contrast)).

Functional groups of synthesized materials were analyzed by Fourier transform infrared spectroscopy (FTIR) (Spectrum Two spectrometer (Perkin Elmer, USA)).

Results and discussion

The formation of $MgMn_2O_4$ nanoparticles occurs as a result of the interaction of metal nitrates

and the precipitating agent (NaOH) according to reactions (2)–(6) [12, 15]:

$$Mg(NO_3)_2 + Mn(NO_3)_2 + 4NaOH \rightarrow \rightarrow Mg(OH)_2 + Mn(OH)_2 + 4NaNO_3, \quad (2)$$

$$2Mn(OH)_2 + 2OH^- \rightarrow 2Mn(OH)_3 + 2e^-, \quad (3)$$

$$Mg(OH)_2 \leftrightarrow Mg^{2+} + 2OH^-, \quad (4)$$

$$Mn(OH)_3 \leftrightarrow Mn^{3+} + 3OH^-, \quad (5)$$

$$Mg^{2+} + 2Mn^{3+} + 8OH^- \rightarrow MgMn_2O_4 + 4H_2O. \quad (6)$$

The crystal structure and phase purity of the synthesized materials at different calcination temperatures was evaluated using the X-ray diffraction method (Fig. 1).

All diffraction peaks at a calcination temperature of 200 °C corresponded to spinel $MgMn_2O_4$ with a cubic lattice, pronounced crystallinity, and the absence of other phases (Fig. 1). As the calcination temperature increased to 400 °C, the appearance of Mn_5O_8 peaks and a significant increase in the proportion of the amorphous phase were observed in the diffractogram. A further increase in the calcination temperature to 600 °C led to the decomposition of Mn_5O_8 with the formation of Mn_2O_3. However, it should be noted that at calcination temperatures of 400 and 600 °C, the molar fraction of spinel $MgMn_2O_4$ (61.62 and 91.30 %, respectively) significantly exceeded the molar fraction of other phases – Mn_5O_8 (38.38 %) and Mn_2O_3 (8.70 %)) (Table 1).

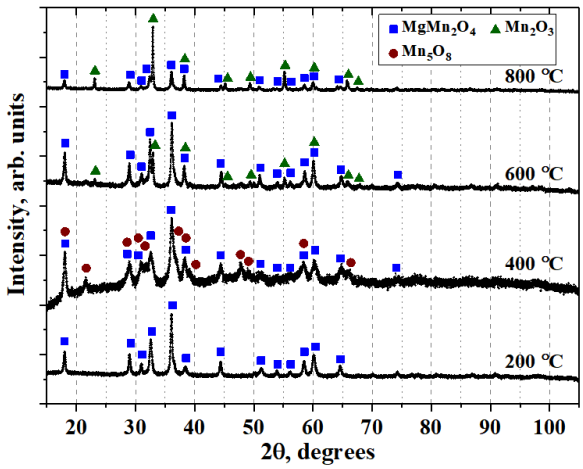

Fig. 1. Diffractograms of materials synthesized by the co-precipitation method in the US field at different calcination temperatures (specific power of ultrasound processing of the reaction medium is 200 W/L)

Table 1

Structural and phase characteristics of materials synthesized using the co-precipitation method in the ultrasound field (specific ultrasound power – 200 W/L)

Calcination temperature, °C	Phase	Mole fraction of the phase, %	Lattice parameters, Å	β, rad.	Cos θ	*D*, nm
200	$MgMn_2O_4$	100.00	*a* = 5.762 (1); *c* = 9.353 (1)	0.005974	0.95075	24.4
400	$MgMn_2O_4$	61.62	*a* = 5.764 (1); *c* = 9.340 (1)	0.010645	0.95078	13.7
	Mn_5O_8	38.38	*a* = 10.368 (3); *b* = 5.738 (2) – angle = 109.73 (2) deg.; *c* = 4.876 (1)	0.012504	0.96887	11.4
600	$MgMn_2O_4$	91.30	*a* = 5.752 (1); *c* = 9.407 (1)	0.005589	0.95065	26.1
	Mn_2O_3	8.70	*a* = 9.400 (1)	0.003632	0.95891	39.8
800	$MgMn_2O_4$	54.34	*a* = 5.757 (1); *c* = 9.416 (1)	0.005964	0.95073	24.5
	Mn_2O_3	45.66	*a* = 9.399 (1)	0.003508	0.95889	41.2

At a calcination temperature of 800 °C, the ratio of spinel mole fractions $MgMn_2O_4$ (54.34 %) and Mn_2O_3 (45.66 %) was significantly lower than at lower calcination temperatures.

Therefore, with an increase in the calcination temperature, the intensity of spinel decomposition into individual oxides increased. This is also confirmed by the EDAX results. Thus, even at a calcination temperature of 400 °C, a violation of the stoichiometric composition of $MgMn_2O_4$ spinel was recorded, which consisted of an increase in the mass or atomic fractions of Mn and O due to the formation

of Mn_5O_8 (Fig. 2; Table 2). Therefore, 200 °C was chosen as the rational value of the calcination temperature at which a single-phase system ($MgMn_2O_4$ spinel) was obtained.

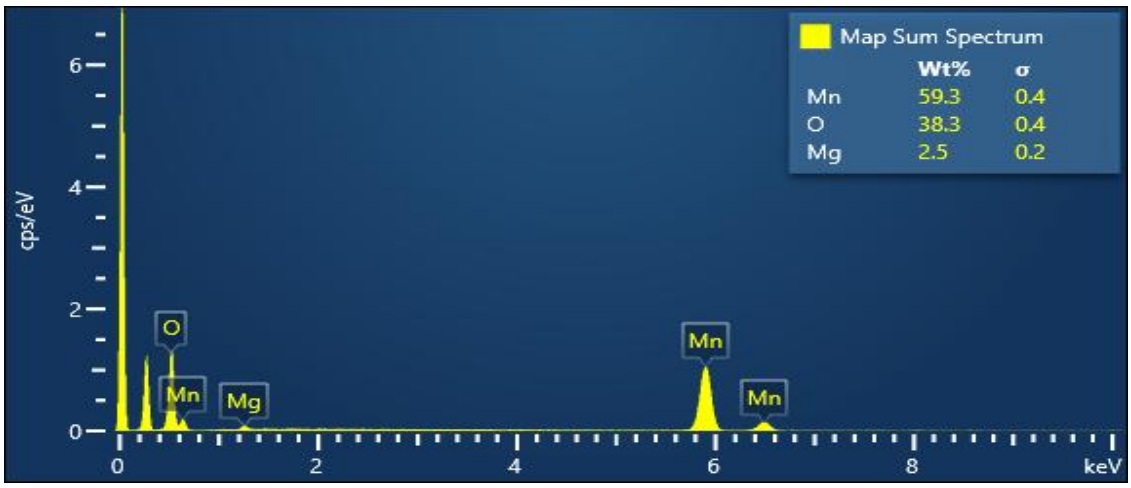

Fig. 2. EDAX spectrum of the material synthesized using the co-precipitation method in the US field (calcination temperature – 400 °C)

Table 2

Comparison of the elemental composition of the synthesized sample (based on the results of the EDAX method) with the stoichiometric composition of spinel $MgMn_2O_4$

Element	Material synthesized by the co-precipitation method in US field		$MgMn_2O_4$ spinel of stoichiometric composition	
	composition, % wt.	composition, % at.	composition, % wt.	composition, % at.
Mg	2.5	2.8	12.1	14.3
Mn	59.3	30.2	55.6	28.6
O	38.2	67.0	32.3	57.1

The main structural and phase characteristics (qualitative and quantitative composition of phases, crystal lattice parameters, average size of crystallites) of the samples synthesized by co-precipitation method in the ultrasound field are given in Table 1. The average size of $MgMn_2O_4$ particles obtained at a calcination temperature of 200 °C was 24.4 nm. At higher calcination temperatures, the average size of $MgMn_2O_4$ particles, calculated from diffraction peaks using the Debye – Scherrer equation, was in the range of 13.7–26.1 nm.

Based on the analysis of SEM images of $MgMn_2O_4$ particles (Fig. 3) and the EDAX maps of the spinel (Fig. 4), it was established that $MgMn_2O_4$ nanoparticles are evenly distributed, uniform in size and morphology (their shape is spherical), but agglomerated. As the calcination temperature of the samples increased, the tendency to agglomeration of nanosized $MgMn_2O_4$ particles also increased. This can be explained by the strengthening of the interaction between particles with magnetic properties, in particular between particles of Mn oxides [14].

The FTIR spectrum of spinel $MgMn_2O_4$ (Fig. 5) was recorded in the range of wave numbers 400–4000 cm^{-1}. The analysis of this spectrum shows the presence of peaks at 473 and 600 cm^{-1}, indicating the valence vibrations of Mg–O and Mn–O, respectively. Peaks at 1635 and 3348 cm^{-1} correspond to valence vibrations of hydroxyl groups of adsorbed water and hydroxyl groups on the surface of $MgMn_2O_4$.

The influence of the specific power of the ultrasonic processing of the reaction medium on the size of $MgMn_2O_4$ spinel particles was determined based on the results of calculations based on diffractograms (Fig. 6).

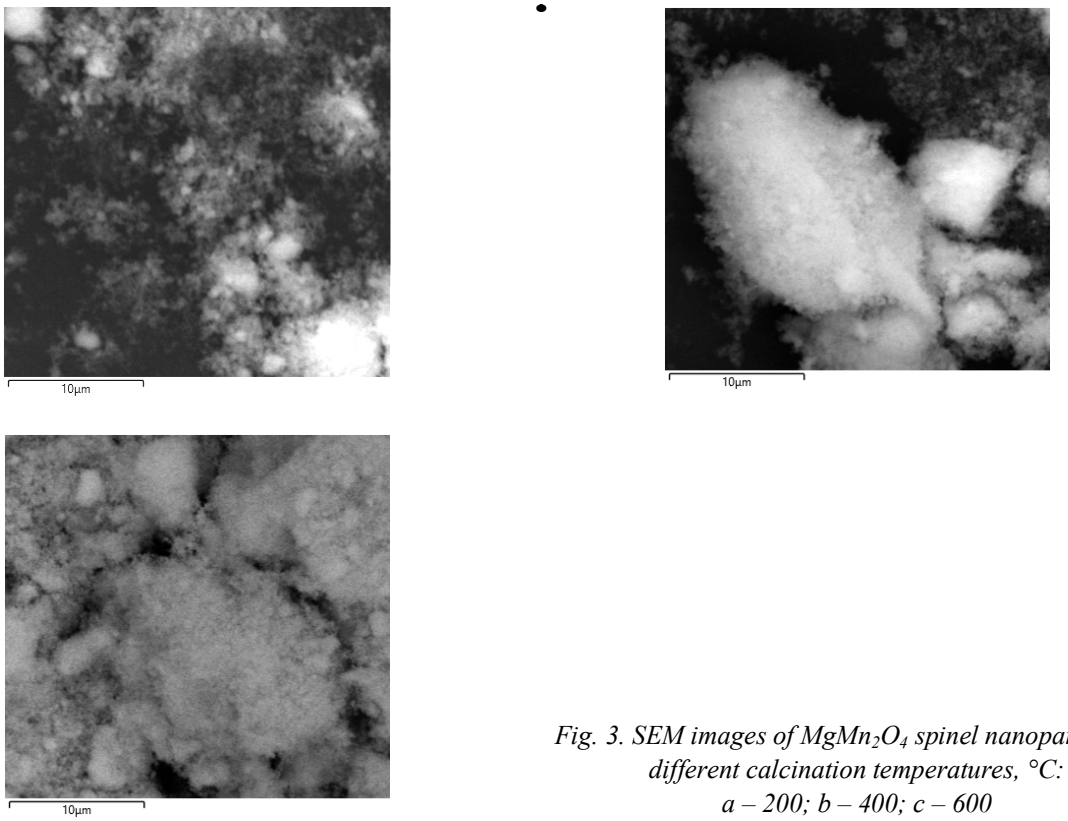

Fig. 3. SEM images of $MgMn_2O_4$ spinel nanoparticles at different calcination temperatures, °C: a – 200; b – 400; c – 600

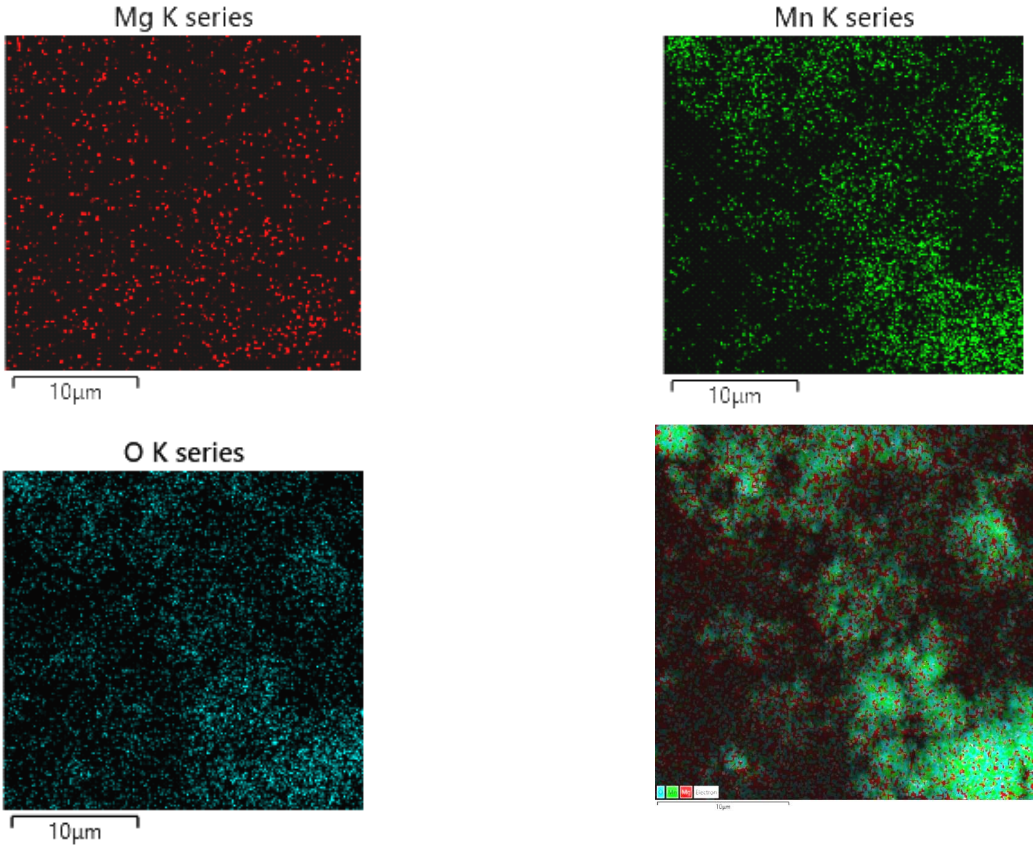

Fig. 4. EDAX maps of $MgMn_2O_4$ spinel (calcination temperature – 200 °C)

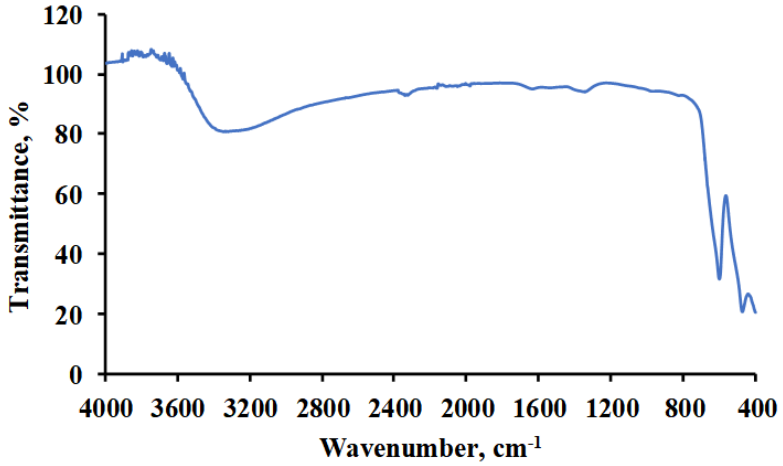

Fig. 5. FTIR spectrum of $MgMn_2O_4$ spinel (calcination temperature – 200 °C)

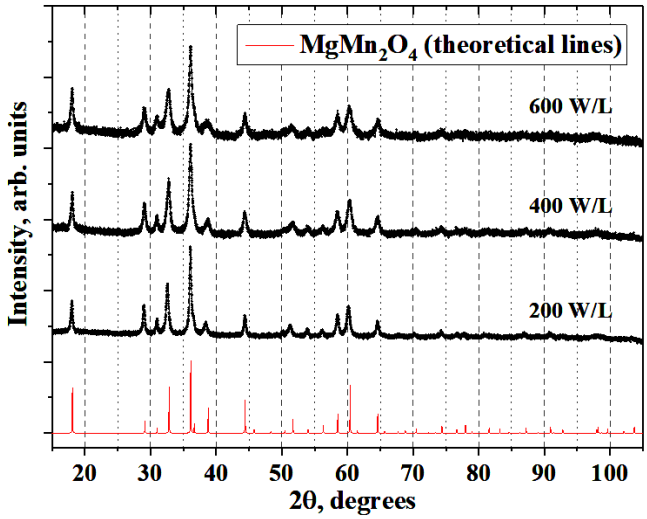

Fig. 6. Diffractograms of $MgMn_2O_4$ spinel synthesized by co-precipitation method at a different specific power of US processing of the reaction medium

Table 3

The influence of the specific power of the ultrasonic processing of the reaction medium on the average size of $MgMn_2O_4$ spinel particles synthesized by the co-precipitation method in the ultrasonic field

Specific power of US processing, W/L	Lattice parameters, Å	β, rad.	cosθ	*D*, nm
200	a = 5.762 (1); c = 9.353 (1)	0.005974	0.95075	24.4
400	a = 5.768 (1); c = 9.298 (1)	0.008457	0.95081	17.2
600	a = 5.766 (1); c = 9.306 (1)	0.009521	0.95078	15.3

As the specific power of ultrasonic processing of the reaction medium increased, the proportion of the amorphous phase increased (Fig. 6), and the average size of $MgMn_2O_4$ particles naturally decreased (Table 3). This was caused by the intensification of the dispersive effect of the ultrasound with an increase in its power.

Conclusions

$MgMn_2O_4$ spinel particles were synthesized by co-precipitation method in the ultrasonic field. X-ray diffraction, energy dispersive X-ray analysis, scanning electron microscopy, and Fourier transform infrared spectroscopy were used to characterize the synthesized particles. It was established that at a calcination

temperature of 200 °C, all peaks on the diffractogram of the synthesized material corresponded to spinel $MgMn_2O_4$ with a cubic lattice, pronounced crystallinity, and the absence of other phases. With an increase in the calcination temperature, the formation of new phases – Mn oxides (respectively, Mn_5O_8 and Mn_2O_3) – was recorded, which is due to the decomposition of the spinel. The average size of $MgMn_2O_4$ particles obtained at a calcination temperature of 200 °C was 24.4 nm.

Based on the analysis of SEM images of $MgMn_2O_4$ particles and EDAX maps of the spinel, it was found that $MgMn_2O_4$ nanoparticles are evenly distributed, uniform in size and morphology (their shape is spherical), but agglomerated. As the calcination temperature of the samples increased, the tendency to agglomeration of nanosized $MgMn_2O_4$ particles increased. This can be explained by the strengthening of the interaction between particles with magnetic properties, in particular between particles of Mn oxides.

An increase in the specific power of ultrasonic processing of the reaction medium from 200 to 600 W/L led to an increase in the proportion of the amorphous phase and a decrease in the average size of $MgMn_2O_4$ particles (calcination temperature – 200 °C) from 24.4 to 15.3 nm.

Authors acknowledge the funding of Ministry of Education and Science of Ukraine for scientific research project of young scientists "Advanced oxidation processes, including nanocatalytic, based on cavitation technologies for purification of aqueous media from resistant N-substituted organic compounds" (state registration number 0122U000790).

This study was conducted using devices of the Centre of Collective Use of Scientific Equipment: "Laboratory of Perspective Technologies of Creation and Physico-Chemical Analyses of New Substances and Functional Materials" at Lviv Polytechnic National University (https://lpnu.ua/ckkno).

References

1. Yu, J., Qiu, W., Lin, X., Wang, Y., Lu, X., Yu, Y., …Ma, J. (2023). Periodate activation with stable $MgMn_2O_4$ spinel for bisphenol A removal: Radical and non-radical pathways. *Chemical Engineering Journal*, *459*, 141574. DOI: 10.1016/j.cej.2023.141574

2. Iranmanesh, P., Saeednia, S., Mehran, M., & Rashidi Dafeh, S. (2017). Modified structural and magnetic properties of nanocrystalline $MnFe_2O_4$ by pH in capping agent free co-precipitation method. *Journal of Magnetism and Magnetic Materials*, *425*, 31–36. DOI: 10.1016/j.jmmm.2016.10.105

3. Akhlaghi, N., & Najafpour-Darzi, G. (2021). Manganese ferrite ($MnFe_2O_4$) nanoparticles: From synthesis to application – A review. *Journal of Industrial and Engineering Chemistry*, 103, 292–304. DOI: 10.1016/j.jiec.2021.07.043

4. Chaudhari, A., Kaida, T., Desai, H. B., Ghosh, S., Bhatt, R. P., & Tanna, A. R. (2022). Dye degradation and antimicrobial applications of manganese ferrite nanoparticles synthesized by plant extracts. *Chemical Physics Impact*, *5*, 100098. doi: 10.1016/j.chphi.2022.100098

5. Rodiah, S., & Ramadhani, E. (2022). Highly efficient removal of methylene blue dye from wastewater using CaO–$MnFe_2O_4$ nanoparticles prepared with teak leaf extract. *Al Kimiya: Jurnal Ilmu Kimia dan Terapan*, 9(2), 62–67. DOI: 10.15575/ak.v9i2.20068

6. Thao, L. T., Nguyen, T. V., Nguyen, V. Q., Phan, N. M., Kim, K. J., Huy, N. N., & Dung, N. T. (2023). Orange G degradation by heterogeneous peroxymonosulfate activation based on magnetic $MnFe_2O_4$/α-MnO_2 hybrid. *Journal of Environmental Sciences*, *124*, 379–396. DOI: 10.1016/j.jes.2021.10.008

7. Jacintha, A. M., Umapathy, V., Neeraja, P., & Rajkumar, S. R. J. (2017). Synthesis and comparative studies of $MnFe_2O_4$ nanoparticles with different natural polymers by sol-gel method: structural, morphological, optical, magnetic, catalytic and biological activities. *Journal of Nanostructure in Chemistry*, *7*, 375–387. DOI: 10.1007/s40097-017-0248-z

8. Liu, H., Dai, X., Kong, L., Sui, C., Nie, Z., Liu, Y., ...Zhan, J. (2023). Ball milling treatment of Mn_3O_4 regulates electron transfer pathway for peroxymonosulfate activation. *Chemical Engineering Journal*, *467*, 143339. DOI: 10.1016/j.cej.2023.143339

9. Sui, C., Nie, Z., Liu, H., Boczkaj, G., Liu, W., Kong, L., & Zhan, J. (2024). Singlet oxygen-dominated peroxymonosulfate activation by layered crednerite for organic pollutants degradation in high salinity wastewater. *Journal of Environmental Sciences*, *135*, 86–96. DOI: 10.1016/j.jes.2023.01.010

10. Wu, S., Qin, H., Cheng, H., Shi, W., Chen, J., Huang, J., & Li, H. (2022). A novel $MnFe_2O_4$-HSO_3 nanocatalyst for heterogeneous Fenton degradation of antibiotics. *Catalysis Communications*, *171*, 106522. DOI: 10.1016/j.catcom.2022.106522

11. Qin, H., Yang, Y., Shi, W., & She, Y. (2021). Heterogeneous Fenton degradation of ofloxacin catalyzed by magnetic nanostructured $MnFe_2O_4$ with different mor-

phologies. *Environmental Science and Pollution Research*, *28*, 26558–26570. DOI: 10.1007/s11356-021-12548-y

12. Junlabhuta, P., Nuthongkuma, P., & Pechrapab, W. (2018). Influences of calcination temperature on structural properties of $MnFe_2O_4$ nanopowders synthesized by co-precipitation method for reusable absorbent materials. *Materials Today: Proceedings*, *5*(6), 13857–13864. DOI: 10.1016/j.matpr.2018.02.028

13. Ghatreh-Samani, R., & Mostafaei, A. (2014). Chemical co-precipitation synthesis of spinel manganese ferrite nanoparticles ($MnFe_2O_4$): Morphological characterizations and magnetic properties. *Journal of Magnetism and Magnetic Materials*, 11.005. DOI: 10.1016/j.jmmm.2014.11.005

14. Aghrich, K., Mtougui, S., Goumrhar, F., Abdellaoui, M., Mamouni, N., Fekhaoui, M., …Mounkachi, O. (2022). Experimental and theoretical investigation of the synthesis, electronic and magnetic properties of $MnFe_2O_4$ spinel ferrite. *Energies*, *15*, 8386. DOI: 10.3390/en15228386

15. Rafique, M. Y., Li-Qing, P., Javed, Q., Iqbal, M. Z., Hong-Mei, Q., Farooq, M. H., & Tanveer, M. (2013). Growth of monodisperse nanospheres of $MnFe_2O_4$ with enhanced magnetic and optical properties. *Chinese Physics B*, *22*(10), 107101. DOI: 10.1088/1674-1056/22/10/107101

16. Yavors'kyi, V. T., Znak, Z. O., Sukhats'kyi, Y. V., Mnykh, R. V. (2017). Energy characteristics of treatment of corrosive aqueous media in hydrodynamic cavitators. *Materials Science*, *52*(4), 595–600. DOI: 10.1007/s11003-017-9995-8

Ю. В. Сухацький[1], М. А. Созанський[2], М. В. Шепіда[1], З. О. Знак[1], С. В. Хом'як[3]
Національний університет "Львівська політехніка",
[1] кафедра хімії і технології неорганічних речовин,
[2] кафедра фізичної, аналітичної та загальної хімії,
[3] кафедра технології біологічно активних сполук, фармації та біотехнології

СИНТЕЗ НАНОЧАСТИНОК ШПІНЕЛІ $MgMn_2O_4$ МЕТОДОМ СПІВОСАДЖЕННЯ В УЛЬТРАЗВУКОВОМУ ПОЛІ

Методом співосадження в ультразвуковому полі синтезовано наночастинки шпінелі $MgMn_2O_4$. Встановлено, що за температури кальцинації 200 °С усі піки на дифрактограмі синтезованого матеріалу відповідали шпінелі $MgMn_2O_4$ з кубічною решіткою, вираженою кристалічністю та відсутністю інших фаз. З підвищенням температури кальцинації зафіксовано утворення нових фаз – оксидів Mn (відповідно, Mn_5O_8 і Mn_2O_3). За дифракційними піками з використанням рівняння Дебая – Шеррера розраховано середній розмір частинок $MgMn_2O_4$, який за температури кальцинації 200 °С дорівнював 24,4 нм. Виявлено закономірне збільшення частки аморфної фази і зменшення середнього розміру частинок $MgMn_2O_4$ зі збільшенням питомої потужності ультразвукового оброблення реакційного середовища.

Ключові слова: шпінель; наночастинки; метод співосадження; ультразвукове поле; рівняння Дебая – Шеррера; середній розмір кристаліту.